



Published in final edited form as:

Nat Commun. 2013 ; 4: 1590. doi:10.1038/ncomms2594.

## Engineering the type III secretion system in non-replicating bacterial minicells for antigen delivery

Heather A. Carleton, María Lara-Tejero, Xiaoyun Liu, and Jorge E. Galán\*

Department of Microbial Pathogenesis, Yale University School of Medicine, 295 Congress Avenue, New Haven, CT 06536, USA

### Abstract

Type III protein secretion systems are being considered for vaccine development since virtually any protein antigen can be engineered for delivery by these nanomachines into the class I antigen presentation pathway to stimulate antigen-specific CD8<sup>+</sup> T cells<sup>12</sup>. A limitation in the use of this system is that it requires live virulence-attenuated bacteria, which may preclude its use in certain populations such as children and the immunocompromised. Here we report the engineering of the *Salmonella* Typhimurium type III secretion system in achromosomal, non-replicating nanoparticles derived from bacterial minicells. The engineered system is shown to be functional and capable of delivering heterologous antigens to the class I antigen presentation pathway stimulating immune responses both *in vitro* and *in vivo*. This antigen delivery platform offers a novel approach for vaccine development and cellular immunotherapy.

### Introduction

Efficient vaccines must not only stimulate innate immune receptors, but also deliver antigens to specific subcellular compartments so that they can be processed via the class I and class II antigen-presenting pathways resulting in the production of antigen-specific cytotoxic T cells and antibodies<sup>3</sup>. Live replicating pathogenic bacteria, such as *Salmonella* Typhimurium, rendered avirulent and engineered with the ability to express foreign antigens are being considered as vaccine vectors to protect against various infectious diseases or as therapeutic agents against cancer<sup>4-6</sup>. Although they potently stimulate innate immune receptors, one limitation of these bacterial vaccine platforms is their inefficient capacity to stimulate cytotoxic T cell responses<sup>7,8</sup>, which require the delivery of antigens to the cytosol of antigen presenting cells. This limitation has been largely overcome by the use of type III secretion systems (T3SS)<sup>2,9</sup>, which are complex multi-protein molecular machines that deliver bacterial virulence effector proteins into the host cell cytosol<sup>10</sup>. Proteins destined to travel the T3SS pathway possess discrete signals that direct them to the secretion machine<sup>11</sup>. When incorporated into heterologous proteins, these signals can target virtually any protein

Users may view, print, copy, download and text and data- mine the content in such documents, for the purposes of academic research, subject always to the full Conditions of use: [http://www.nature.com/authors/editorial\\_policies/license.html#terms](http://www.nature.com/authors/editorial_policies/license.html#terms)

\*For correspondence: jorge.galan@yale.edu; Phone: 203-7372404; Fax: 203-7372630.

**Competing interests:** The authors declare no competing interests

**Author contributions:** HC, ML-T, XL, and JEG designed and carried out experiments; HC and JEG wrote the manuscript with comments from all authors; JEG directed the project.

for delivery through this secretion pathway<sup>2,12</sup>. Consequently, T3SS have been engineered to deliver heterologous antigens in the context of virulence attenuated bacterial pathogens<sup>9</sup>. Heterologous protein antigens delivered by this system have been shown to stimulate antigen specific CD8<sup>+</sup> T-cells, which in animal models conferred protection to a variety of infectious diseases or caused the regression of established tumors<sup>9,13-22</sup>. A second limitation of the virulence-attenuated bacterial vaccine platforms relates to their safety. Residual virulence of the attenuated pathogen or the potential for virulence-reversion may limit their use in certain populations such as children or the immunocompromised.

To overcome some of the limitations of virulence-attenuated bacterial antigen delivery vectors while retaining some of its benefits, we sought to engineer the T3SS in a non-replicating antigen-delivery platform. Since protein translocation by T3SSs requires energy provided by ATP hydrolysis and a proton gradient<sup>23</sup>, the use of this system has been restricted to the context of live virulence-attenuated bacteria. The intrinsic complexity of the assembly of this large, multi-protein machine combined with its energy requirements, virtually preclude the development of a synthetic platform capable of supporting the function of T3SS. As an alternative to a synthetic platform, we sought to engineer bacterial minicells with the capacity to deliver heterologous proteins through the *Salmonella* Typhimurium T3SS encoded within its pathogenicity island 1 (SPI-1). Bacterial minicells result from aberrant cell division and although they lack chromosomal DNA they have the capacity to synthesize proteins and sustain a proton gradient<sup>24</sup>. In addition, these nanoparticles have immune adjuvant capacity<sup>25</sup> since they retain most of the bacterial components capable of stimulating innate immune receptors<sup>26</sup>. We report here the assembly of a functional type III secretion system in bacterial minicells and its use for antigen delivery.

## Results

### Bacterial minicells assemble type III secretion systems

We isolated minicells from a *S. Typhimurium* strain carrying a deletion mutation in *minD* (Supplementary Fig. S1), which is required for proper cell division<sup>27</sup>. Loss of this gene results in aberrant cell division with the production of a large number of minicells (Fig. 1a). We examined by LC-MS/MS highly purified minicell preparations for the presence of components of the SPI-1 T3SS. While we were able to detect most of the SPI-1 T3SS components (Fig. 1b and Supplementary Table S1), the concentrations of T3SS-associated proteins were significantly lower compared to that of the originating bacterial cells. In particular, the protein translocases, which mediate the passage of the type III secreted proteins through the mammalian cell membrane<sup>28</sup>, were significantly depleted in bacterial minicells. These results were confirmed by western blot analysis of selected T3SS-associated proteins (Fig. 1c, Supplementary Figures S2 and S3a). These findings indicated that although components of the SPI-1 T3SS can partition into minicells, they might not be abundant enough to efficiently function as a protein delivery machine. To increase the levels of SPI-1 T3SS components partitioned into minicells we introduced into the *S. Typhimurium minD* strain a plasmid encoding HilA, the positive transcription regulator of the SPI-1 T3SS, expressed under a rhamnose-inducible promoter<sup>29</sup>. Previous studies have

shown that the overexpression of HilA results in increased levels of all components of this system. LC-MS/MS analysis of minicells produced by this strain showed significantly increased levels of SPI-1 T3SS components (Fig. 1b and 1c, Supplementary Fig. S2, S3a and Supplementary Table S2). Consistent with these findings, minicells assembled T3SS needle complexes, the core structure of this secretion machine<sup>30</sup>, which could be readily visualized by electron microscopy in intact minicells (Fig. 1d) or in purified needle complex preparations (Fig. 1e). These results indicate that SPI-1 T3SS components not only can partition into minicells but also can assemble into a potentially functional secretion machine.

### Minicells assemble functional type III secretion systems

A functional SPI-1 T3SS machine must be able to deploy the protein translocases SipB, SipC, and SipD, which will eventually mediate the passage of the secreted proteins through the mammalian cell membrane<sup>28</sup>. Prior to contact with host cells, only SipD, a component of the needle tip complex, is displayed on the bacterial surface<sup>31</sup>. To probe for the presence of potentially functional T3SS complexes, we examined minicells by immunofluorescence microscopy for the presence of surface-localized SipD. We found that a significant proportion of minicells isolated from bacterial cells overexpressing HilA displayed SipD on their surface (Fig. 2a and 2b). In contrast, minicells isolated from a SPI-1 T3SS-defective mutant did not (Fig. 2a and 2b). These results indicate that minicells assemble T3SS complexes potentially competent for protein translocation into mammalian cells.

Minicells are metabolically active and capable of synthesizing *de novo* plasmid-encoded proteins after the partitioning of plasmids into minicells<sup>24</sup>. We therefore tested whether purified minicells were competent for the secretion and translocation into cultured mammalian cells of a *de novo* synthesized SPI-1 T3SS effector protein. Minicells were isolated from T3SS-competent or T3SS-defective strains carrying a plasmid which encodes the effector protein SopB<sup>32</sup> expressed from an arabinose-inducible promoter. Isolated minicells were incubated in the presence of arabinose for 3 hours and the secretion of SopB to culture medium was assessed by Western immunoblot analysis. SopB was detectable in supernatants of T3SS-competent minicells but not from supernatants of T3SS-defective minicells despite equivalent amount of SopB in lysates of whole minicells obtained from either strain (Fig. 2c and Supplementary Fig. S3b). One of the characteristic features of some T3SSs such as the one encoded by the *S. Typhimurium* SPI-1 is that their activity is stimulated upon contact with eukaryotic cells<sup>33</sup>. Consistent with this behavior, we found greater levels of secreted SopB upon exposure of minicells to cultured Henle-407 epithelial cells (Fig. 2d). We also examined the ability of minicells to inject proteins to cultured epithelial cells using a fractionation protocol previously developed in our laboratory to detect translocated effector proteins in the cytosol of infected cells<sup>28</sup>. We found detectable levels of translocated SopB in preparation of cultured cells exposed to minicells obtained from wild-type *S. Typhimurium* but not in those exposed to minicells obtained from a SPI-1 T3SS-defective mutant (Fig. 2e). These results indicate that minicells assemble a functional T3SS capable of mediating protein secretion and translocation into eukaryotic cells.

### T3SS in minicells can deliver antigen *in-vitro*

It has been previously shown that live, virulence-attenuated *S. Typhimurium* can deliver heterologous antigens in a T3SS-dependent manner to the major class I antigen presentation pathway<sup>9</sup>. To determine whether the T3SS in minicells was also capable of such delivery, the first 104 amino acids of SopE, containing the T3SS-targeting signal<sup>20</sup>, were fused to 16 amino acids of the OVA antigen containing the class I restricted SIINFEKL peptide<sup>34</sup> along with a C-terminal 3×FLAG tag (SopE-OVA) (Fig. 3a). A plasmid encoding this chimeric protein was introduced into minicell-producing T3SS-competent or T3SS-defective *S. Typhimurium* strains (Fig. 3b and Supplementary Fig. S3c). We then tested the ability of minicells to deliver SopE-OVA in a T3SS-dependent manner to the class I antigen-presenting pathway. Murine RMA cells were incubated with minicells purified from different parental strains and the ability of the RMA cells to present the class I restricted OVA peptide to the class I-restricted B3Z T-cell reporter<sup>35</sup> was assayed by measuring β-galactosidase production by the reporter cells. Minicells purified from T3SS-competent *S. Typhimurium* were found to efficiently deliver SopE-OVA to RMA cells (Fig. 3c). In contrast, minicells obtained from a T3SS-defective mutant were not (Fig. 3c). These results demonstrate that minicells are capable of T3SS-dependent translocation of an effector-antigen construct. In addition, these results indicate that minicell T3SS-delivered effector-antigen constructs can elicit a MHC class I restricted immune response and activation of CD8<sup>+</sup> T-cells *in vitro*.

Although purified minicells were shown to be capable of delivering antigen in a T3SS-dependent manner, the efficiency of delivery was relatively poor. We reasoned that this inefficiency might be at least partially due to the lower levels of some critical components of the T3SS in minicells. Secretion of proteins through the T3SS requires customized cytoplasmic chaperones, which target them to the secretion machinery<sup>10</sup>. Since proteomic analysis indicated that the partitioning of the SopE chaperone InvB (as well as other T3SS chaperones) into minicells was inefficient (Supplementary Table S1), we added *invB* to the plasmid expressing the chimeric *sopE-OVA* construct that partitions into minicells. Expression of *invB* in tandem with *sopE-OVA* improved the relative antigen presentation of minicells by over 2-fold (Fig. 3c). The proteomics analysis also showed that the translocases SipB, SipC, and SipD and their associated chaperones InvE and SicA were also depleted in minicells (Supplementary Table S1). Consequently, we added to the expression plasmid the genes encoding these proteins. Although expression of the antigen construct was slightly lower (Fig. 3b and Supplementary Fig. S3c), minicells obtained from this strain showed a significantly higher antigen presenting ability, achieving a level essentially equivalent to that of the peptide positive control (Fig. 3c). These results show that the T3SS-mediated antigen delivery by purified minicells can be optimized by the expression of T3SS components encoded by plasmids that can partition into minicells.

Dendritic cell (DC) immunotherapy is emerging as a promising strategy for autologous treatment of infectious diseases and cancer<sup>36</sup>. Some configurations of this strategy involve the *ex-vivo* antigen loading of autologous DCs prior to their application back to the recipients. Minicells could potentially offer advantages for *ex-vivo* loading of DCs since not only they can deliver antigen to the class I antigen presenting pathway, essential in anti-

tumor immune responses, but also they can potentially deliver DC maturation signals through the Toll-receptor agonists present in these nanoparticles. We therefore tested whether minicells could deliver antigen to DCs *ex vivo*. Mouse bone marrow-derived DCs were incubated with minicells obtained from strains carrying a plasmid expressing *sopE-OVA* along with its chaperone *invB* and the protein translocases and their chaperones (Fig. 3d and Supplementary Fig. S3d). Antigen loading was assayed by measuring the ability of dendritic cells to present the class I restricted OVA peptide to the class I-restricted allogeneic B3Z T-cell reporter cell. We found that the response elicited by the minicell-pulsed DCs in the reporter cell line was equivalent to the peptide positive control (Fig. 3e). Antigen presentation was strictly dependent on the presence of the T3SS in the minicells since DCs pulsed with equivalent number of minicells obtained from a T3SS-deficient bacterial strain did not elicit a response in the reporter cell line (Fig. 3d and 3e and Supplementary Fig. 3d). These results show that minicells can effectively deliver antigen to DCs *ex vivo*.

### T3SS in minicells can prime CD8<sup>+</sup> T-cell responses *in vivo*

We evaluated the potential of minicells expressing SopE-OVA to prime CD8<sup>+</sup> T-cell responses *in vivo*. OT-I CD8<sup>+</sup> T-cells (CD45.2), which can specifically recognize an OVA epitope<sup>37</sup>, were adoptively transferred into C57BL/6J congenic mice expressing CD45.1. Recipient mice were then immunized with purified minicells optimized for the delivery of SopE-OVA by co-expressing the chaperone InvB and the translocases. As controls, mice were immunized with minicells obtained from a T3SS-defective strain expressing SopE-OVA or minicells obtained from a T3SS-competent strain that did not express SopE-OVA (Fig. 4a and Supplementary Fig. S3e). After three weeks, the recipient mice were boosted with recombinant VSV-OVA and 5 days after the boost mice were sacrificed and the expansion of OT-I CD8<sup>+</sup> T-cells was analyzed. Mice immunized with minicells purified from the wild-type parental vaccine strain expressing SopE-OVA had a significant expansion of the CD45.2 CD8<sup>+</sup> donor OT-I T-cells specific for the OVA peptide (Fig. 4b). In contrast, mice immunized with minicells expressing SopE-OVA purified from a T3SS-defective background or minicells lacking SopE-OVA, did not show expansion of the adoptively transferred OT-I CD8<sup>+</sup> T-cells upon boosting with VSV-OVA (Fig. 4b). These results indicate that minicells can prime antigen-specific CD8<sup>+</sup> T-cell responses *in vivo* in a T3SS-dependent manner.

We also evaluated the ability of minicells to elicit a protective immune response in a mouse model of *Listeria monocytogenes* infection. We stimulated *ex vivo* bone-marrow derived dendritic cells with minicells expressing a chimera consisting of the secretion and translocation domain of SopE fused to *Listeria monocytogenes* MHC class I restricted immunogenic peptides from listeriolysin O and p60 (SopE-Lis) (Fig. 4c), which have been shown to induce protective CD8<sup>+</sup> T-cell responses in Balb/c mice<sup>38,39</sup>. For controls, dendritic cells were stimulated *ex vivo* with purified minicells obtained from a T3SS-defective strain expressing SopE-Lis or minicells obtained from a T3SS-competent strain that did not express SopE-Lis (Fig. 4d and Supplementary Fig. S3f). Stimulated dendritic cells were then transferred by tail vein injection into recipient mice, and 6 days after the transfer, recipient mice were challenged with *L. monocytogenes*. Three days after challenge,

mice were sacrificed and the c. f. u. of *Listeria monocytogenes* in the spleens were enumerated. We found significantly lower number of c. f. u. in the spleens of mice that had received dendritic cells stimulated with T3SS-competent minicells expressing the *L. monocytogenes* antigens than in the control animals (Fig. 4e). These results demonstrate that dendritic cells stimulated *ex vivo* by T3SS-competent minicells can confer protection from an infectious challenge.

## Discussion

We have described here a strategy to engineer the *S. Typhimurium* T3SS into nanoparticles capable of delivering antigens directly into the cytosol of antigen presenting cells to stimulate the production of protective, antigen-specific class I-restricted CD8<sup>+</sup> T-cells. The development of these nanoparticles expands the potential of the T3SS as an antigen delivery platform of heterologous antigens by providing a safer, non-replicating vehicle for vaccination against infections in which this type of response is crucial for protection. In addition, this system may provide an effective strategy to prime dendritic cells *ex vivo* for immunotherapy against infectious diseases and cancer.

## Methods

### Bacterial strains and growth conditions

All bacterial strains used in this study are derivatives of *Salmonella enterica* serovar Typhimurium (*S. Typhimurium*) SL1344 and are listed in Supplementary Table S3. The *minD*:*cat* mutant allele was introduced into *S. Typhimurium* as previously described<sup>40</sup>. All plasmids used in this study were constructed using standard recombinant DNA techniques and are detailed in Supplementary Table S4. All *S. Typhimurium* strains were grown in Luria broth (LB) containing 0.3 M NaCl to induce the expression of the T3SS encoded on the *Salmonella* pathogenicity island -1 (SPI-1).

### Minicell purification

Minicells were purified using protocols adapted from previously published methods<sup>24</sup> with several modifications (Supplementary Fig. S1). Briefly, a 500 ml culture of a *minD*:*cat* mutant strain was grown under low aeration and agitation until an OD at A<sub>600</sub> of 1.1 was reached. Minicells were subsequently enriched in a series of two low-speed centrifugations at 2,000 g in which the supernatants were collected while the pellets containing mostly bacterial rods were discarded. Minicells were recovered by a final centrifugation for 30 min at 10,000g, resuspended in a solution of buffered saline gelatin (BSG) and applied to the top of a continuous 5-20% iodixanol (OptiPrep™, Axis-Shield PLC, Scotland) density gradient formed using the gradient forming function of the Gradient Station™ (Biocomp Instruments; Fredericton, NB, Canada) in SW28 (Beckman Coulter) tubes. Gradients were subjected to 20 min of centrifugation at 2,000g in a Beckman Coulter ultracentrifuge. After centrifugation, minicell-enriched fractions were collected using the fraction collection feature of the Gradient Station™ (Biocomp Instruments; Fredericton, NB, Canada) in 1.5 ml aliquots. Minicells in the different fractions were pelleted at 18,000g and resuspended in the appropriate buffer for further usage. Minicells suspended in glycerol were enumerated using



DIC microscopy on a CELL-VU® disposable slide that contains a chamber of a known depth of 20µm. The number of contaminating rods in the purified minicell fractions was determined by counting the colony forming units of serial dilutions of the different fractions. The outlined protocol yielded minicells with a diameter of 200 to 550 nm (with an average of  $394 \pm 90$  nm). The average yield of purified minicells was  $1.67 \pm 0.70 \times 10^{12}$  minicells per preparation. The contamination from bacterial rods was estimated to be 1 rod in  $10^6$  minicells, which represents 0.001 % of the total protein mass present in the minicell preparation (Supplementary Fig. S4). This low level of contaminating rods did not impact any of the assays conducted with minicells since proteins potentially secreted by these number of rods would be well below detection in secretion (Supplementary Fig. S5) or antigen presentation (Supplementary Fig. S6) assays.

### **SDS-Polyacrylamide Gel Electrophoresis and Immunoblotting**

Lysates were solubilized in Laemmli buffer and then separated on sodium dodecyl sulfate (SDS)-10% or 15% polyacrylamide gels. The gels were subsequently visualized by Coomassie brilliant blue staining. For immunoblotting, proteins were transferred onto PVDF or nitrocellulose membranes and treated with mouse monoclonal antibodies against the relevant proteins or epitope tags as indicated (Supplementary Table S5). Protein bands were visualized using an Odyssey infrared imaging system (LI-COR Biosciences). When comparing protein concentrations between different samples by immunoblot, all samples were first normalized to the detected integrated intensity of cell lysates after Coomassie blue staining using the Odyssey infrared imaging system (Supplementary Fig. S3).

### **Mass spectrometry analysis**

Equivalent protein concentrations of minicell and bacterial rod proteins from a parental strain grown under SPI-1 T3SS-inducing conditions were briefly separated on a 10% SDS-PAGE gel and processed for liquid chromatography–tandem mass spectrometry (LC-MS/MS) to identify peptides as previously described<sup>41</sup>. See Supplementary Methods for additional details on data analysis.

### **Electron microscopy**

Minicells were purified from bacterial rods grown under SPI-1 T3SS-inducing conditions. After purification, the minicells were subsequently osmotically-shocked and visualized under the electron microscope following a protocol adapted from Kubori et al.<sup>30</sup>.

### **Immunofluorescence staining**

Purified minicells were isolated from bacterial rods grown to an optical density measured at 600 nm (OD<sub>600</sub>) of 1.1. These minicells were serially diluted and spun at 750g onto acid washed, poly-D lysine coated coverslips and fixed for 30 min in a 4% paraformaldehyde solution in PBS. Coverslips were washed and incubated with a solution of 3% bovine serum albumin in PBS for 30 min. Minicells were subsequently labeled with rabbit polyclonal anti-S. Typhimurium lipopolysaccharide (Difco Laboratories) at a 1:2,000 dilution or mouse monoclonal anti-Flag M2 (Sigma) at a 1:10,000 dilution for 1 hour. Minicells were then labeled with secondary anti-rabbit antibody conjugated to Alexa 594, an anti-mouse

antibody conjugated to Alexa 488 at a dilution of 1:2,000, and DAPI. Images were captured with a fluorescence microscope (Nikon Diaphot) equipped with a Princeton Instruments CCD camera and analyzed using ImageJ (U. S. National Institutes of Health, Bethesda, Maryland, USA). The proportion of minicells expressing SipD on their surface was determined after overlaying captured images showing the LPS stain, the SipD stain, and the DIC image of the minicells. For each minicell sample, three different experiments (i.e. biological replicates) were used for immunofluorescence analysis and two different fields of view were analyzed per biological replicate counting a minimum of 4,000 minicells for each condition.

### Analysis of T3SS function in bacterial minicells

Minicells were purified from a strain carrying plasmids expressing SopB and its chaperone SigE under the control of an arabinose-inducible promoter (*pBAD-sopB-sigE*) and <sup>42</sup> a plasmid expressing HilA. Purified minicells were then incubated for 3 hours at 37°C in the presence of the 0.1% arabinose to allow further expression of the SopB construct. Minicells were subsequently pelleted at 20,000× g for 30 min at 4° C, supernatants removed and filtered through a 0.22 µm-pore-size filter to remove any remaining minicells. Proteins from this supernatant were precipitated by adding 0.1% sodium deoxycholate and 10% trichloroacetic acid. After incubation at 4° C overnight, proteins were recovered by centrifugation at 20,000g for 20 min. Pellets were washed in acetone, dried and resuspended in Laemmli buffer. Polyacrylamide gel electrophoresis and Western blot analysis of the recovered supernatant proteins was carried out as described above.

Minicell-mediated protein translocation into cultured cells was assayed as previously described <sup>28</sup> with some modifications. Purified minicells were added to Henle-407 cells grown to ~80% confluency in 15cm tissue culture dishes in the presence of the proteasome inhibitor MG132 (to prevent effector protein degradation) and 0.2% arabinose. After 2.5 hours treatment, the supernatant and extracellular minicells were removed and centrifuged at 8,000 × g for 30 min at 4° C, the supernatant was collected and filtered through a 0.22 µm-pore-size filter to remove any remaining minicells. Henle-407 cells were washed with PBS 3 times and scraped off the plates in the presence of 5 µM protease inhibitors and 0.1% Triton-X 100. The Triton-X 100 insoluble fraction was resuspended in Laemmli buffer and proteins in the extracellular supernatant and Triton-X 100 soluble fraction were precipitated by addition of ammonium sulfate (50% weight/vol final concentration), resuspended in 10M Urea, and analyzed by Western blot analysis.

### Antigen presentation assay

Analysis of antigen delivery and subsequent CD8<sup>+</sup> T-cell activation was carried out using an *in vitro* T cell activation assay adapted from previously published protocols <sup>2,35</sup> with minor modifications detailed in the Supplementary Methods.

### Adoptive transfer and animal immunization

Adoptive transfer experiments were carried out as previously described<sup>43</sup> with minor modification detailed in the Supplementary Methods. For protection studies, BMDCs were prepared from Balb/c mice as outlined above, and incubated in the presence of GM-CSF



with purified minicells prepared from different bacterial strains, all carrying the *asd* mutation (to prevent replication of the minor contaminating bacterial rod fraction). The BMDCs were extensively washed and applied in the tail vein of Balb/c recipient mice. Six days after BMDC transfer, mice were challenged i. v. with  $7 \times 10^3$  cfus *Listeria monocytogenes* strain 10403s and sacrificed 3 days later. Spleens were removed from the sacrificed mice and c. f. u. enumerated by plating dilutions of homogenized tissues.

### Measurement of OVA-specific CD8<sup>+</sup> T-cell responses

Splenocytes prepared from immunized mice were resuspended in PBS containing 0.1% BSA and added to a 96-well U-bottom plates at a concentration of  $1-2 \times 10^6$  cells in 50 $\mu$ l per well. Splenocytes were then stained with conjugated antibodies directed at CD8 (FITC) and CD45.2 (APC), using standard procedures at 4°C (conjugated antibodies from eBioscience). Stained cells were fixed in 2.5% formaldehyde in PBS at 4°C overnight and analyzed using a FACSCalibur flow cytometer (Becton-Dickson) and FlowJo software (Tree Star, Inc.). All animal experiments were carried out in accordance with and have been approved by the Institutional Animal Care and Use Committee of Yale University.

### Supplementary Material

Refer to Web version on PubMed Central for supplementary material.

### Acknowledgments

We thank Dr. Leo Lefrancois for providing VSV-OVA and members of the Galán laboratory for critical reading of this manuscript. This work was supported by NIH Grant AI30492 to J. E. G. and a Grant from the Grand Challenges Program of the Gates Foundation to J. E. G.

### References

1. Russmann H, et al. Delivery of epitopes by the Salmonella type III secretion system for vaccine development. *Science*. 1998; 281:565–568. [PubMed: 9677200]
2. Chen LM, Briones G, Donis RO, Galan JE. Optimization of the delivery of heterologous proteins by the Salmonella enterica serovar Typhimurium type III secretion system for vaccine development. *Infect Immun*. 2006; 74:5826–5833.10.1128/IAI.00375-06 [PubMed: 16988261]
3. Amanna I, Slifka M. Contributions of humoral and cellular immunity to vaccine-induced protection in humans. *Virology*. 2011; 411:206–215. [PubMed: 21216425]
4. Curtiss, Rr, et al. New technologies in using recombinant attenuated Salmonella vaccine vectors. *Crit Rev Immunol*. 2010; 30:255–270. [PubMed: 20370633]
5. Hegazy W, Hensel M. Salmonella enterica as a vaccine carrier. *Future Microbiol*. 2012; 7:111–127. [PubMed: 22191450]
6. Moreno M, Kramer M, Yim L, Chabalgoity J. Salmonella as live trojan horse for vaccine development and cancer gene therapy. 2010; 10:56–76. 56–76.
7. Gao XM, et al. Recombinant *Salmonella typhimurium* strains that invade nonphagocytic cells are resistant to recognition by antigen-specific cytotoxic T lymphocytes. *Infect Immun*. 1992; 60:3780–3789. [PubMed: 1500187]
8. Yang DM, et al. Oral *Salmonella typhimurium* (AroA-) vaccine expressing a major leishmanial surface protein (gp63) preferentially induces T helper 1 cells and protective immunity against leishmaniasis. *J Immunol*. 1990; 145:2281–2285. [PubMed: 2144549]
9. Russmann H, et al. Delivery of epitopes by the Salmonella type III secretion system for vaccine development. *Science*. 1998; 281:565–568. [PubMed: 9677200]

10. Galan JE, Wolf-Watz H. Protein delivery into eukaryotic cells by type III secretion machines. *Nature*. 2006; 444:567–573. [PubMed: 17136086]
11. Arnold R, Jehl A, Rattei T. Targeting effectors: the molecular recognition of Type III secreted proteins. *Microbes Infect*. 2010; 12:346–358. [PubMed: 20178857]
12. Michiels T, Cornelis GR. Secretion of hybrid proteins by the *Yersinia* Yop export system. *J Bacteriol*. 1991; 173:1677–1685. [PubMed: 1999387]
13. Russmann H, et al. Protection against murine listeriosis by oral vaccination with recombinant *Salmonella* expressing hybrid *Yersinia* type III proteins. *J Immunol*. 2001; 167:357–365. [PubMed: 11418671]
14. Wieser A, Magistro G, Nörenberg D, Hoffmann C, Schubert S. First multi-epitope subunit vaccine against extraintestinal pathogenic *Escherichia coli* delivered by a bacterial type-3 secretion system (T3SS). *International Journal of Medical Microbiology*. 2012; 302:10–18. [PubMed: 22000741]
15. Zhu X, et al. Tumor antigen delivered by *Salmonella* III secretion protein fused with heat shock protein 70 induces protection and eradication against murine melanoma. *Cancer Science*. 2010; 101:2621–2628. [PubMed: 20880334]
16. Chamekh M. Immunomodulation using genetically engineered bacteria for type III-mediated delivery of heterologous antigens and cytokines: Potential application in vaccine and therapeutical developments. *Immunopharmacology and Immunotoxicology*. 2010; 32:1–4. [PubMed: 19778176]
17. Tartz S, et al. Complete protection against *P. berghei* malaria upon heterologous prime/boost immunization against circumsporozoite protein employing *Salmonella* type III secretion system and *Bordetella* adenylate cyclase toxoid. *Vaccine*. 2008; 26:5935–5943. [PubMed: 18804138]
18. Sevil Domènech V, Panthel K, Winter S, Rüssmann H. Heterologous prime-boost immunizations with different *Salmonella* serovars for enhanced antigen-specific CD8 T-cell induction. *Vaccine*. 2008; 26:1879–1886. [PubMed: 18313813]
19. Konjufca V, Wanda S, Jenkins M, Curtiss R III. A recombinant attenuated *Salmonella enterica* serovar typhimurium vaccine encoding *Eimeria acervulina* antigen offers protection against *E. acervulina* challenge. *Infection and Immunity*. 2006; 74:6785–6796. [PubMed: 16982843]
20. Evans DT, et al. Mucosal Priming of SIV-specific CTL Responses in Rhesus Macaques by the *Salmonella* Type III Secretion Antigen Delivery System. *J Virol*. 2003; 77:2400–2409. [PubMed: 12551977]
21. Kotton CN, et al. Safety and immunogenicity of attenuated *Salmonella enterica* serovar Typhimurium delivering an HIV-1 Gag antigen via the *Salmonella* Type III secretion system. *Vaccine*. 2006; 24:6216–6224. [PubMed: 16824652]
22. Nishikawa H, et al. In vivo antigen delivery by *Salmonella typhimurium* type III secretion system for therapeutic cancer vaccine. *J Clin Inv*. 2006; 116:1946–1954.
23. Galán J. Energizing type III secretion machines: what is the fuel? *Nat Struct Mol Biol*. 2008; 15:127–128. [PubMed: 18250631]
24. Frazer A, C R 3rd. Production, properties and utility of bacterial minicells. *Curr Top Microbiol Immunol*. 1975; 69:1–84. [PubMed: 1098854]
25. Giacalone M, et al. Immune responses elicited by bacterial minicells capable of simultaneous DNA and protein antigen delivery. *Vaccine*. 2006; 24:6009–6017. [PubMed: 16806602]
26. Palm N, Medzhitov R. Pattern recognition receptors and control of adaptive immunity. *Immunol Rev*. 2009; 227:221–233. [PubMed: 19120487]
27. de Boer P, Crossley R, Rothfield L. A division inhibitor and a topological specificity factor coded for by the minicell locus determine proper placement of the division septum in *E. coli*. *Cell*. 1989; 56:641–649. [PubMed: 2645057]
28. Collazo C, Galán JE. The invasion-associated type III system of *Salmonella typhimurium* directs the translocation of Sip proteins into the host cell. *Mol Microbiol*. 1997; 24:747–756. [PubMed: 9194702]
29. Bajaj V, Hwang C, Lee CA. *hilA* is a novel *ompR*.*toxR* family member that activates the expression of *Salmonella typhimurium* invasion genes. *Mol Microbiol*. 1995; 18:715–727. [PubMed: 8817493]
30. Kubori T, et al. Supramolecular structure of the *Salmonella typhimurium* type III protein secretion system. *Science*. 1998; 280:602–605. [PubMed: 9554854]

31. Lara-Tejero M, Galan JE. The Salmonella Typhimurium SPI-1 type III secretion translocases mediate intimate attachment to non-phagocytic cells. *Infect Immun.* 2009; 77:2635–2642. [PubMed: 19364837]
32. Galyov EE, et al. A secreted effector protein of Salmonella dublin is translocated into eukaryotic cells and mediates inflammation and fluid secretion in infected ileal mucosa. *Mol Microbiol.* 1997; 25:1903–1912.
33. Zierler MK, Galan JE. Contact with cultured epithelial cells stimulates secretion of Salmonella typhimurium invasion protein InvJ. *Infect Immun.* 1995; 63:4024–4028. [PubMed: 7558314]
34. Dick LR, et al. Proteolytic processing of ovalbumin and beta-galactosidase by the proteasome to a yield antigenic peptides. *Journal of Immunology.* 1994; 152:3884–3894.
35. Karttunen J, Sanderson S, Shastri N. Detection of rare antigen-presenting cells by the lacZ T-cell activation assay suggests an expression cloning strategy for T-cell antigens. *Proc Natl Acad Sci U S A.* 1992; 89:6020–6024. [PubMed: 1378619]
36. Tacke P, de Vries I, Torensma R, Figdor C. Dendritic-cell immunotherapy: from ex vivo loading to in vivo targeting. *Nat Rev Immunol.* 2007; 7:790–802. [PubMed: 17853902]
37. Hogquist K, et al. T cell receptor antagonist peptides induce positive selection. *Cell.* 1994; 76:17–27. [PubMed: 8287475]
38. Harty JT, Bevan MJ. CD8+ T cells specific for a single nonamer epitope of Listeria monocytogenes are protective in vivo. *J Exp Med.* 1992; 175:1531–1538. [PubMed: 1375265]
39. Harty JT, Pamer E. CD8 T Lymphocytes Specific for the Secreted p60 Antigen Protect Against listeria monocytogenes Infection. *J Immunol.* 1995; 154:4642–4650. [PubMed: 7722316]
40. Kaniga K, Bossio JC, Galán JE. The *Salmonella typhimurium* invasion genes *invF* and *invG* encode homologues to the PulD and AraC family of proteins. *Mol Microbiol.* 1994; 13:555–568. [PubMed: 7997169]
41. Lara-Tejero M, Kato J, Wagner S, Liu X, Galan JE. A sorting platform determines the order of protein secretion in bacterial type III systems. *Science.* 2011; 331:1188–1191.10.1126/science.1201476 [PubMed: 21292939]
42. Patel JC, Hueffer K, Lam TT, Galan JE. Diversification of a Salmonella virulence protein function by ubiquitin-dependent differential localization. *Cell.* 2009; 137:283–294.10.1016/j.cell.2009.01.056 [PubMed: 19379694]
43. Ripoll A, et al. In vitro selection of variants resistant to beta-lactams plus beta-lactamase inhibitors in CTX-M beta-lactamases: predicting the in vivo scenario? *Antimicrob Agents Chemother.* 2011; 55:4530–4536.10.1128/AAC.00178-11 [PubMed: 21788458]

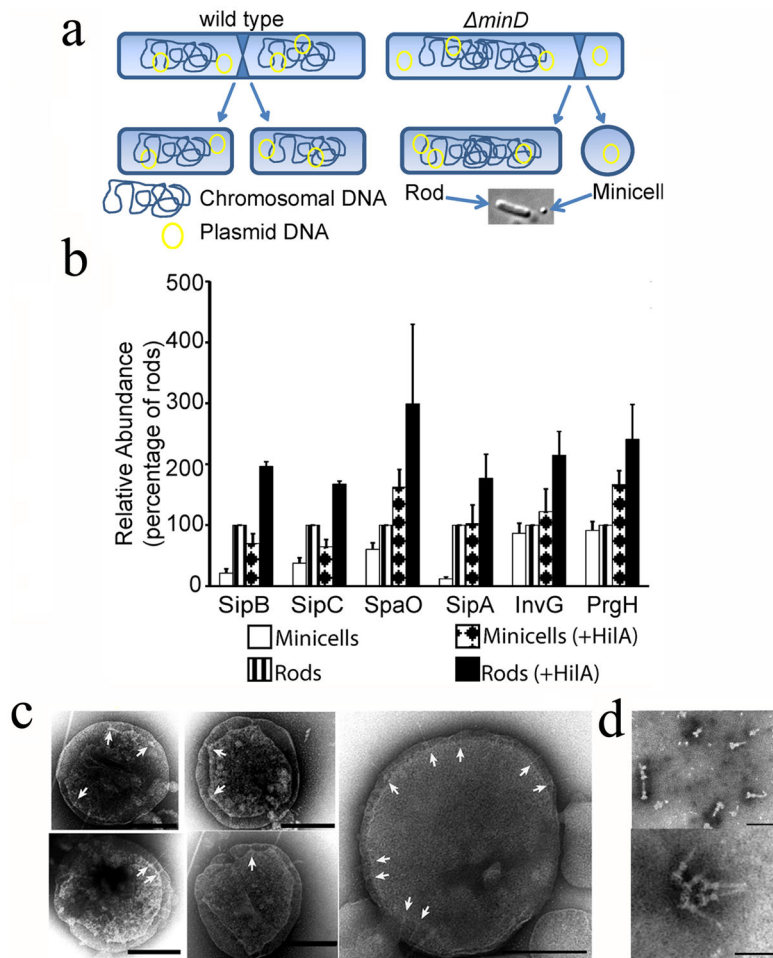


**Fig. 1. Bacterial minicells assemble a type III secretion system**

(a) Schematic of minicell generation (see also Supplementary Fig. S1). (b) Relative abundance of selected T3SS proteins analyzed by immunoblotting. Values are standardized compared to those obtained from wild-type *S. Typhimurium* rods and normalized according to the total protein concentration of each sample. Values are the mean  $\pm$  standard deviation of 3 independent measurements. See additional information in Materials and Methods and Supplementary Fig. S2 and S3. (c) Electron micrographs of negatively-stained osmotically-shocked minicells. Arrows indicate T3SS needle complexes on the minicell envelope. Scale bars: 200 nm. (d) Electron micrographs of negatively-stained needle complexes isolated from purified minicells. Scale bars: 100 nm (top) and 50 nm (bottom).

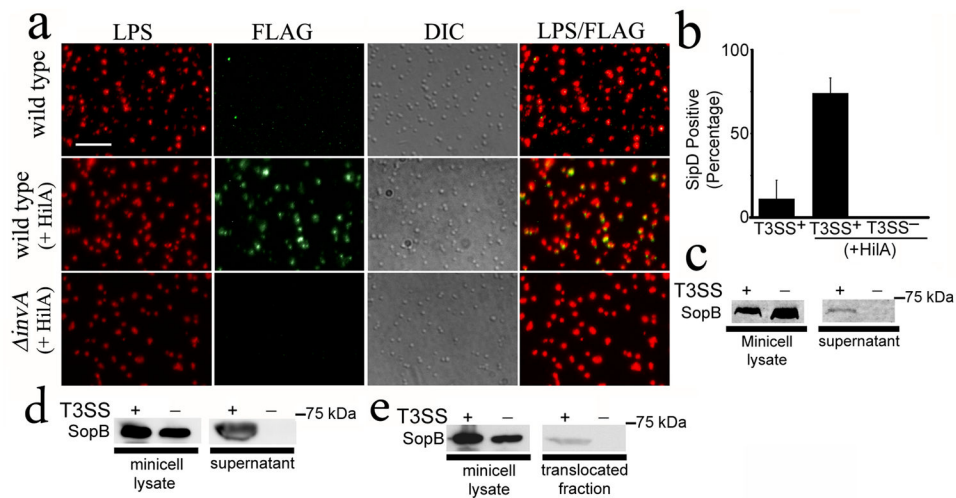


**Fig. 2. The type III secretion system in minicells is functional**

(a and b) Detection of the needle complex tip protein SipD on the surface of purified minicells. Minicells were isolated from wild-type or T3SS-defective (*invA*) *S. Typhimurium* strains expressing SipD-FLAG and carrying a plasmid expressing the SPI-1 T3SS positive transcriptional regulator HilA. Minicells were stained with an antibody to LPS (red), an antibody against the FLAG tag (green), and examined by immunofluorescence and DIC microscopy. Scale bar: 2.5  $\mu$ m (a). The % of minicells showing surface SipD stain is shown (b). Values represent the mean  $\pm$  standard deviation of three independent experiments in which a minimum of 4,000 cells per strain were counted. (c) and (d) Secretion of *de novo* synthesized effector proteins by purified minicells through their SPI-1 T3SS. Minicells were isolated from wild type or T3SS-defective (*invA*) *S. Typhimurium* strains carrying a plasmid encoding the SPI-1 T3SS effector SopB expressed under the control of an arabinose-inducible promoter. Isolated minicells were incubated for 3 hs in the presence of arabinose and the presence of SopB in minicell lysates and supernatants were analyzed by western blot (c). Alternatively, minicells were exposed to cultured Henle-407 cells and the presence of SopB in supernatants examined as described above (d). (e) Minicell-mediated, type III secretion dependent protein translocation into cultured epithelial cells. Henle-407 cells were treated with minicells isolated from type III secretion competent or type III secretion-defective (*invA*) as described above and added to Henle-407 cells for 2.5hs. The presence of the effector protein SopB in minicell lysates and the translocated fraction was assayed by Western blot.

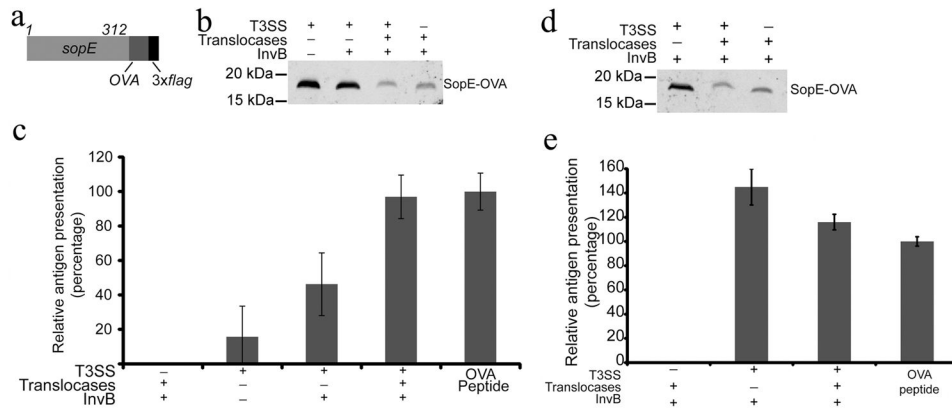


**Fig. 3. T3SS-dependent antigen delivery by micells *in-vitro***

**(a)** Schematic of the SopE-OVA construct used in these studies. **(b)** Western blot analysis of micells obtained from wild type or T3SS-defective ( *invA*) *S. Typhimurium* strains expressing the SopE-OVA construct and used in the experiment shown in **(c)**. When indicated, the SopE-OVA construct was co-expressed with the SopE chaperone InvB and the T3SS protein translocases and their chaperones to improve protein secretion and/or translocation. Equal amount of total protein was loaded in each sample. **(c)** Analysis of antigen delivery by micells to antigen-presenting cells. RMA cells (C57BL/6 mouse hybridomas) were pulsed for 3 hs with micells isolated from wild type or T3SS-defective ( *invA*) *S. Typhimurium* strains. After pulsing, RMA cells were fixed, and used as APCs in a B3Z T-cell activation assay as described in experimental procedures. Values represent the levels of antigen presentation based on the  $\beta$ -galactosidase activity detected in the B3Z-T cell hybridoma reporter and are normalized relative to the values of the OVA peptide positive control, which was considered 100 %. The values are the mean  $\pm$  standard deviation of three independent experiments. **(d and e)** Micells can deliver antigen to dendritic cells *ex vivo*. **(d)** Western blot analysis of micells obtained from wild type or T3SS-defective ( *invA*) *S. Typhimurium* strains expressing the SopE-OVA construct and used in the experiment shown in **(e)**. Equal amount of total protein was loaded in each sample. **(e)** Bone marrow-derived dendritic cells were pulsed for 3 hs with micells isolated from the indicated *S. Typhimurium* strains carrying a plasmid expressing SopE-OVA and the indicated SPI-1 T3SS-associated proteins. After pulsing, dendritic cells were fixed and used as APCs in a B3Z T-cell activation assay as described in Supplementary Materials. Values represent the levels of antigen presentation based on the  $\beta$ -galactosidase activity detected in the B3Z-T cell hybridoma reporter and they are normalized relative to the values of the OVA peptide positive control, which was considered 100 %. The values are the mean  $\pm$  standard deviation of three independent experiments.



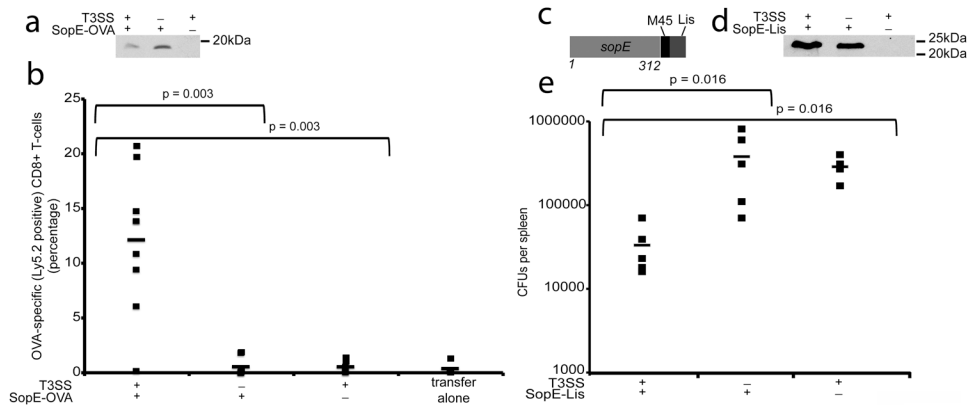


**Fig. 4. T3SS-dependent priming of protective CD8<sup>+</sup> T-cell responses by micinells**

**(a)** Western blot analysis of micinells obtained from wild type or T3SS-defective (*invA*) *S. Typhimurium* strains expressing the SopE-OVA construct and used in the experiment shown in **(b)**. Equal amount of total protein was loaded in each sample. **(b)** Splenocytes from OT-I mice were adoptively transferred into recipient mice (C57BL/6/CD45.1), which were subsequently immunized with micinells isolated from the indicated *S. Typhimurium* *asd* strains expressing SopE-OVA. Three weeks after micinell immunization mice were boosted and the levels of OVA-specific CD8<sup>+</sup> T cells were measured by flow cytometry as indicated in Materials and Methods. Values represent the percentage of OVA-specific CD8<sup>+</sup> T-cells in each individual mouse (number of mice used in each category: T3SS<sup>+</sup>/SopE-OVA<sup>+</sup>: 9; T3SS<sup>-</sup>/SopE-OVA<sup>+</sup>: 7; T3SS<sup>+</sup>/SopE-OVA<sup>-</sup>: 7; 4 transfer alone: 4). Data were analyzed using the Student's t test. **(c)** Schematic of SopE-Lis construct used in the protection experiments. **(d)** Western blot analysis of micinells obtained from wild type or T3SS-defective (*invA*) *S. Typhimurium* strains expressing the SopE-Lis construct and used in the experiment shown in **(e)**. **(e)** BMDCs prepared from Balb/c mice were incubated with micinells isolated from the indicated bacterial strains and transferred by tail vein injection into a Balb/c mouse as indicated in Materials and Methods. Six days after transfer mice were challenged with *L. monocytogenes*, and 3 days after challenge the c. f. u. in spleens were determined (number of mice used in each category: T3SS<sup>+</sup>/SopE-Lys<sup>+</sup>: 5; T3SS<sup>-</sup>/SopE-Lys<sup>+</sup>: 5; T3SS<sup>+</sup>/SopE-Lys<sup>-</sup>: 4). Data were analyzed using the Wicoxon rank test.

**Table 1**  
**Relative levels of T3SS-associated proteins in purified minicells**

TTSS Protein	Relative Abundance <sup>1</sup>	
	minicells vs rods	minicells (+HilA vs wt)
<i>Regulatory proteins</i>		
HilA	-1.8	67
HilD	0.4	ND
IacP	-1.3	ND
InvF	-3.4*	9.6
<i>Structural and associated proteins</i>		
InvA	-0.9	12
InvC	-3.5	14
InvG	-3.5	3
InvH	-3.3	2.1
PrgH	-3.6*	5.1
PrgI	-0.9	ND
PrgJ	-3.3	4.8
PrgK	-3.1	6.0
SpaS	-3.3	-1.9
SpaP	ND	31
<i>Chaperone and chaperone-like proteins</i>		
InvB	-0.13*	2.7
InvE	0.6	2.0
SicA	-1.0*	1.7
SicP	-2.6	14
SigE	-0.8	2.3
SpaO	0.6	3.3
OrgA	-0.3	6.3
OrgB	0.3	4.4
<i>Secreted proteins</i>		
AvrA	-0.1	-1.4
InvJ	-3.6*	-2.8
SipA	-4.0*	2.1
SipB	-1.5	6.3
SipC	-0.2	4.6
SipD	-5.9*	6.2
SlrP	-8.1*	2.9
SopA	-0.8	5.9
SopB	-1.2	2.8
SopD	-3.9	43

Relative Abundance <sup>1</sup>		
TTSS Protein	minicells vs rods	minicells (+HilA vs wt)
<i>Regulatory proteins</i>		
SopE	-0.5	3.4
SopE2	-6.9*	14
SptP	-8.7*	2.1

Author Manuscript

Author Manuscript

Author Manuscript

Author Manuscript